◆ Human Brain Mapping 35:2789–2805 (2014) ◆

Interictal Networks in Magnetoencephalography

Urszula Malinowska,[1,2] Jean-Michel Badier,[1,2] Martine Gavaret,[1,2,3] Fabrice Bartolomei,[1,2,3] Patrick Chauvel,[1,2,3] and Christian-George Bénar[1,2]*

[1]INSERM, UMR 1106, Marseille, France
[2]Aix-Marseille Université, INS, Marseille, France
[3]APHM, Hôpital Timone, Service de neurophysiologie clinique, Marseille, France

Abstract: Epileptic networks involve complex relationships across several brain areas. Such networks have been shown on intracerebral EEG (stereotaxic EEG, SEEG), an invasive technique. Magnetoencephalography (MEG) is a noninvasive tool, which was recently proven to be efficient for localizing the generators of epileptiform discharges. However, despite the importance of characterizing noninvasively network aspects in partial epilepsies, only few studies have attempted to retrieve fine spatiotemporal dynamics of interictal discharges with MEG. Our goal was to assess the relevance of magnetoencephalography for detecting and characterizing the brain networks involved in interictal epileptic discharges. We propose here a semi-automatic method based on independent component analysis (ICA) and on co-occurrence of events across components. The method was evaluated in a series of seven patients by comparing its results with networks identified in SEEG. On both MEG and SEEG, we found that interictal discharges can involve remote regions which are acting in synchrony. More regions were identified in SEEG (38 in total) than in MEG (20). All MEG regions were confirmed by SEEG when an electrode was present in the vicinity. In all patients, at least one region could be identified as leading according to our criteria. A majority (71%) of MEG leaders were confirmed by SEEG. We have therefore shown that MEG measurements can extract a significant proportion of the networks visible in SEEG. This suggests that MEG can be a useful tool for defining noninvasively interictal epileptic networks, in terms of regions and patterns of connectivity, in search for a "primary irritative zone." *Hum Brain Mapp 35:2789–2805, 2014.*

Key words: MEG; intracerebral EEG; SEEG; epilepsy; interictal; connectivity; networks; ICA; presurgical evaluation

INTRODUCTION

The criteria for defining the cortical region to be removed by surgery in order to cure the patient with epilepsy are far from being standardized. In short, they correspond to a compromise solution between the lesion volume as seen by imaging methods (MRI, PET, SPECT…), and the extent of interictal and ictal activities as delineated by electrophysiology. After Bancaud and Talairach's contributions to the concept of "Epileptogenic Zone" [Bancaud and Talairach, 1965; Talairach and Bancaud, 1973], delineation of the seizure onset area has been progressively preferred to the localization of interictal activities as the major criterion to define a surgical strategy. This has been so essentially

Additional Supporting Information may be found in the online version of this article.

Contract grant sponsor: Aix-Marseille Université (to U.M.).

*Correspondence to: Christian-George Bénar, Institut des Neurosciences des Systèmes, UMR 1106, INSERM, Aix-Marseille Université, Faculté de Médecine La Timone, 27 Bd Jean Moulin, 13385 Marseille Cedex 05, France. E-mail: christian.benar@univ-amu.fr

Received for publication 14 February 2013; Revised 11 June 2013; Accepted 17 June 2013.

DOI: 10.1002/hbm.22367

Published online 18 September 2013 in Wiley Online Library (wileyonlinelibrary.com).

because the time scale of a seizure has rendered much more readable its spatio-temporal development through cortical circuits, whereas brevity of interictal spike bursts has constrained to map them as unique focal, transient events. Still, as the conditions of seizure recording may be awkward and the criteria to define the epileptogenic zone not fulfilled in a number of cases, strategies based on parameters of the interictal state need to be developed in order to find alternative and/or complementary ways to determine in practice the cortical area to be resected. These strategies can now be performed thanks to digital signal processing methods, which permit to detect automatically epileptic discharges and extract their spatio-temporal dynamics [Gotman, 1999; Schwartz et al., 2003].

An approach based on interictal discharges could aim at distinguishing among scattered activities those which could characterize a primary irritative zone (i.e., to be resected for a successful surgery) from those arising from a secondary irritative zone [Badier and Chauvel, 1995]. Another interest of using interictal information is to rely on a number of analyzable events much larger than the ictal ones.

In this context, magnetoencephalography (MEG) has proven efficient for non-invasively localizing the generators of interictal epileptiform discharges (IEDs, also called "interictal spikes") [Ebersole, 1997; Fischer et al., 2005; Knowlton et al., 1997; Ossenblok et al., 2007; Schwartz et al., 2003; review in Stefan et al., 2011]. A classical approach consists in selecting visually epileptic spikes, followed by dipole source localization in order to infer the brain generators of the observed signals. This strategy is usually driven by the perspective of finding a "focus," represented by the location of a single equivalent dipole (or clusters of dipoles). However, it has been shown on intracerebral EEG that the implication of networks involving several brain areas is a basic observation for both ictal [Bartolomei et al., 2008; Bartolomei et al., 2001] and interictal activity [Alarcon et al., 1994; Badier and Chauvel, 1995]. In particular, in the case of interictal discharges, it has been proposed to characterize these networks by quantifying the co-occurrences of events across brain structures [Bourien et al., 2005].

Despite the importance of characterizing non-invasively network aspects in partial epilepsies [Gotman, 2008], only few studies have attempted to retrieve their fine spatio-temporal dynamics with non-invasive electrophysiology [Lantz et al., 2003; Merlet et al., 1996; Tanaka et al., 2010].

Our goal in the current study was to assess the capacities of MEG to detect and characterize the brain networks involved in interictal epileptic activity. We propose a semi-automatic method based on independent component analysis (ICA) and on co-occurrence of events across components. The method was evaluated in seven patients who had undergone SEEG by comparing MEG and SEEG identification of interictal networks.

MATERIAL AND METHODS

Patient Selection

We selected seven drug-resistant patients from the Clinical Neurophysiology Department of the Timone Hospital in Marseille, with the following criteria: (i) they had both MEG recordings and intracerebral EEG (Stereotaxic EEG, SEEG) recordings [Talairach and Bancaud, 1973] for presurgical investigation and (ii) MEG recordings were showing stable and frequent interictal spiking. For the MEG recording, informed consent was obtained from each patient. The MEG study was approved by the institutional Review board of INSERM, the French Institute of Health (IRB0000388, FWA00005831).

Before SEEG, these patients had a phase I evaluation including detailed medical history, neurologic examination, video-EEG recording of seizures, structural MRI, interictal and ictal (when possible) single photon emission computed tomography, PET, and neuropsychological evaluation. Following phase I examination, an SEEG investigation was indicated in order to define the epileptogenic zone when it was not possible to make a surgical decision between several hypotheses on the basis of non-invasive data.

Detailed characteristics of patients are given in Table I. In all cases, the MEG exam was performed before surgery. In three cases out of seven, MEG was performed before SEEG during phase I of presurgical evaluation.

MEG Recordings

The biomagnetic signals used in this study were recorded on two systems. The first system is a whole-head 151 gradiometers (CTF Coquitlam, BC, Canada), which was at the time located at la Pitié-Salpêtrière Hospital, Paris. The second machine is a whole-head 248-channel magnetometer system (4D Neuroimaging Inc., San Diego CA), located at la Timone Hospital in Marseille. Each session of acquisition was composed of several runs. Several strategies were used. For patients 3 and 5 (CTF system), the recording was triggered visually on the appearance of spikes, resulting in runs of 20 epochs of 6 s each (2 min). This sampling strategy was used because of disk space constraints at the time of the recording. For patients 4 and 6 (CTF system), each run was composed of three consecutive 100 s sections (5 min). For the other patients (4D systems), the runs were composed of 5 min of continuous recordings. The total number of runs was 20 for the 2 min runs, and ranged from 4 to 7 for the 5 min runs.

The digitization rate was 1,250 Hz on the CTF system and 2,034.5 Hz on the 4D system. The MEG signals were high-pass filtered offline at 1 Hz with a digital filter.

Patients were not hospitalized at the time of the MEG exam; they were under normal medication. There was no seizure before the MEG on the day of acquisition. For one

TABLE I. Summary of clinical findings

Patient	Gender	Age (yr)	Structural MRI	Histology diagnosis	MEG system and date of exam	Date of SEEG	Date of surgery	Surgery	Surgical outcome (ILAE class)
1-ZS	M	25	R parietal FCD	FCD	4D, 05/2009	01/2009	09/2009, gamma knife 2013	R peri-sylvian post cortectomy, gamma-knife (target: right insula)	OC4 (3 yr)
2-DT	M	23	R basal temporo-occipital FCD	—	4D, 07/2009	06/2008	11/2009	Right anterior temporal cortectomy	OC3 (3 yr)
3-GL	F	17	partial corpus callosum agenesis	FCD	CTF, 12/2002	04/2002	05/2003	L prefrontal cortectomy	OC4 (9 yr)
4-LN	F	41	R supracalcarine FCD	—	CTF, 06/2003	03/2006	gamma knife 2006	gamma-knife; R sup calcarine fissure	OC2 (6 yr)
5-BA	F	17	R lateral temporo-occipital FCD	FCD	CTF, 01/2003	05/2003	10/2003	R Lateral occipito-temporal cortectomy	OC4 (9 yr)
6-BC	F	25	L premotor FCD	FCD	CTF, 03/2003	07/2001	01/2005	Left premotor and prefrontal cortectomy	OC4 (7 yr)
7-CA	F	22	R medial and anterior temporal ischemia	Gliosis	4D, 11/2009	11/2009	06/2010	R baso-frontal + anterior temporal cortectomy	OC 3 (2.5 yr)

patient (patient 1), there was a slow rhythmic discharge on one run after that considered for analysis.

SEEG Recordings

Stereoelectroencephalography (SEEG) was performed using multicontact depth electrodes (Alcis, Besançon, France) diameter 0.8 mm, 10 to 15 contacts, length 2 mm, interval 1.5 mm) implanted intracerebrally according to Talairach and Bancaud's stereotaxic method [McGonigal et al., 2007; Talairach and Bancaud, 1973]. For each patient, 6 to 11 electrodes were implanted, providing more than 100 contacts of measurement in each case and sampling the brain areas of interest. The placement of electrodes was determined by the clinical, neurophysiological, and anatomical characteristics of each patient. The sampling frequency of SEEG signals was 512 Hz. We analyzed one hour of SEEG for each patient. This section of data was selected during the second day of SEEG recordings, distant from the anesthesia period and at least two hours away from a seizure. Moreover, we used a daytime recording in order to avoid potential confound effects that could arise from comparing daytime MEG signals with sleep SEEG recordings.

The precise location of each electrode was determined by co-registering the post-implantation MRI and the implantation CT scan showing the electrodes. The co-registration was linear, relying on landmarks placed manually on the two images (MedInria software, www-sop.inria.fr/asclepios/software/MedINRIA/index.php).

MEG Signal Processing

Independent component analysis (ICA)

Independent component analysis [Comon, 1994], or ICA, is a method for separating multivariate signals into additive components, assuming statistical independence of the source signals. Each independent component (IC) is composed of a spatial pattern (topography at the sensor level) and a corresponding time course. ICs are chosen to produce maximally temporally independent signals. Here, the infomax ICA [Bell and Sejnowski, 1995] was used for decomposition of continuous epochs (5 min or 2 min), without any a priori information on spike occurrence. We chose to analyze only two runs for each patient, in the beginning of the session. Dimensionality reduction was performed by singular value decomposition (SVD) before ICA computation, resulting in a dimension of 30. This dimension was chosen based on the profile of singular values resulting from the SVD analysis of a representative dataset. We used the runica function of the EEGLAB software [Delorme and Makeig, 2004]. Computation was performed on a PC, on Matlab 64 bits with 8 Gb of RAM. At the end of the runica procedure, components were ranked by energy of the signals reconstructed at the sensor level (i.e., projected with the mixing matrix).

Spikes detection and selection of components

In order to identify ICA components related to epileptic spikes, an automatic detection algorithm as proposed by Bourien et al. was used [Bourien et al., 2004, 2005] based on the Page-Hinkley approach [Page, 1954]. The algorithm permits a detection of transient signals, which results in an increase of energy in the 20–40 Hz band, as well as an estimation of the actual start of events [see Bourien et al., 2004 for details of implementation]. Thresholds were tuned manually on a 20 s window of data for each patient based on visual inspection. This semi-automated detection resulted in a distribution of the number of spikes across ICA components. We selected components presenting both (i) a large number of spikes and (ii) topographies consistent with brain activity (i.e. presenting dipolar topographies indicative of one or several dipolar sources) [Delorme et al., 2012].

Co-occurrence testing

Following the principles of Bourien et al. [2005] developed for intracerebral interictal spikes, we counted for all pairs of ICs the spikes which were co-occurring on a short time window ($L = 100$ ms length). We note the sets of detections in component $j \in \{1,2\}$ as $S_j = \left\{ t_1^j, \ldots, t_{n_j}^j \right\}$, with n_j number of detections in component j. The number of co-occurring spikes across components i and j is:

$$n_{i\&j} = \text{card}\left\{ (t, t') \in S_i \times S_j \, s.t. \, |t - t'| \leq L \right\} \quad (1)$$

Components with high number of spikes tend to have more co-occurring events, whether this arises by chance or not. We took this factor into account both in the statistics of co-occurrence and in the normalization of co-occurrence values (see below).

For each pair of components, we tested the significance of the number of co-occurring spikes. A resampling method was used, where the series of inter-spike delays were shuffled for each component independently (100 realizations). This permitted to estimate the null distribution corresponding to "no significant co-occurrence." The threshold was found on the empirical histogram (significance level of 0.05, using a Bonferroni correction for multiple comparisons). This procedure preserves the number of spikes in each component: a pair of components with high number of spikes in a least one component will result in a high threshold of significance.

For the connectivity graphs, we normalized the absolute number of co-occurrences for a given pair by the maximum number of spikes across the two components i and j:

$$n_{i\&j}^{\text{norm}} = \frac{n_{i\&j}}{\max(n_i, n_j)} \quad (2)$$

This permitted to lower the influence of components with high number of spikes, which can result in a high number of co-occurring events just by chance.

Definition of directionality and leaders

Two tests of directionality were performed in case of significant pair-wise co-occurrence between components.

The simplest measure of directionality is time delay. Therefore, we tested first the temporal order across events by a sign test (function signtest.m from Matlab statistics toolbox) performed on the differences of detection times for each event. This "delay test" was thresholded at $P = 0.05$ (not corrected for multiple comparisons).

We designed another measure of directionality based on the probability of occurrences of spikes. If events in component i are strongly linked to spikes in component j, whether events in j can happen independently of events in i, then it can be hypothesized that there is a dependence of j on i [Badier and Chauvel, 1995].

For a given pair of components, we counted the number of independent events (NIE), i.e., spikes seen in one component and not in the other one. The NIE for component i with respect to component j is the number of spikes in i with no corresponding spike in j:

$$\mathrm{NIE}_{i\setminus j} = \mathrm{card}\left\{ t_k^i, k \in 1 \ldots n_i | \forall t_l^j \ , l \in 1 \ldots n_j, |t_l^i - t_k^j| > L \right\} \quad (3)$$

We then computed the ratio R of NIE between components:

$$R_{i \to j} = \frac{\mathrm{NIE}_{i\setminus j}}{\mathrm{NIE}_{j\setminus i}} \quad (4)$$

A high ratio $R_{i \to j}$ was considered as an indication that component i is leading over component j. We considered that a ratio was significant if it was an outlier in the distribution of ratios across all pairs.

We compared the number of ingoing and outgoing connections for each node of the graph (i.e. each component). A given node was defined as leader according to a test (delay or NIE) if at least 90% of connections were outgoing. A node could be marked as a leader according to the delay test, to the NIE test, or to both. When several leaders were pointing towards the same node, we assumed that this reflected indirect connections and we retained only the leader with longer delay or higher number of independent events.

MEG source analysis

Source analysis was performed on the selected ICA components corresponding to epileptic activity. We used the LORETA method [Pascual-Marqui et al., 1994], as implemented in the ASA software (ANT B.V., Enschede, The Netherlands) and the main peak in the LORETA solution for representation. We decided to use maxima of distributed sources instead of single dipoles, as the former was found to be more robust to the presence of small secondary sources.

SEEG Signal Processing

Similar methodology as that used in MEG was applied to SEEG signals (with the exception of ICA decomposition). For each SEEG channel (i.e., contact) the semi-automatic detection of spikes was performed on a bipolar montage under expert control—in order to find the best set of parameters for detection. Next, based on numbers of detected events in each contact, several representative channels (range 9–13) were chosen for further analysis. Selection was made in order to reduce dimensionality (number of channels) by preventing redundancy (signals are often correlated in successive contacts in the same electrode, indicating that these contacts record from the same region). With this in view, one to three representative contacts were selected from each electrode. Selected contacts were chosen as (i) corresponding to local maxima in number of spikes, (ii) sampling deep (contacts 1–3 in 10 contacts electrodes), medium and superficial regions (contacts 7–9 in 10 contacts electrodes), (iii) showing different time courses across representative contacts of the same electrode.

Next, similarly to MEG, significant co-occurrences and directionality of spikes across pairs of selected SEEG channels were determined.

Confrontation of Graphs in MEG and SEEG

Graphs were shown in a three-dimensional rendering of the cortex. The brain mesh was obtained from the patient MRI (Brainvisa software, http://brainvisa.info/index.html). The nodes of the graph were placed at the LORETA peaks for MEG and at the selected contacts for SEEG (in the middle of consecutive contacts of the bipolar montage). In each graph, a line between nodes is shown if co-occurrence of events across the corresponding time courses is significant, and an arrow is added if there is significant directionality.

Each region detected on the graphs was labeled anatomically by an experienced epileptologist (M.G.). Regions were referenced in the sub-lobar brain parcellation classically performed during presurgical evaluation in our clinical department. Regions were matched visually across modalities, and similar regions were presented on the same line of the results table.

RESULTS

ICA and Spike Detection in MEG

Figure 1 presents an extract of the ICA decomposition for one run of MEG (Patient 1), along with the histogram of spike detections across components (Fig. 1c) (only the 20 components with higher energy are shown, out of 30 components in total). Some components are clearly related to artifacts: IC4 to movement artifacts, IC5 to eye blinks, IC11 to ECG. As spike detection is based on the presence

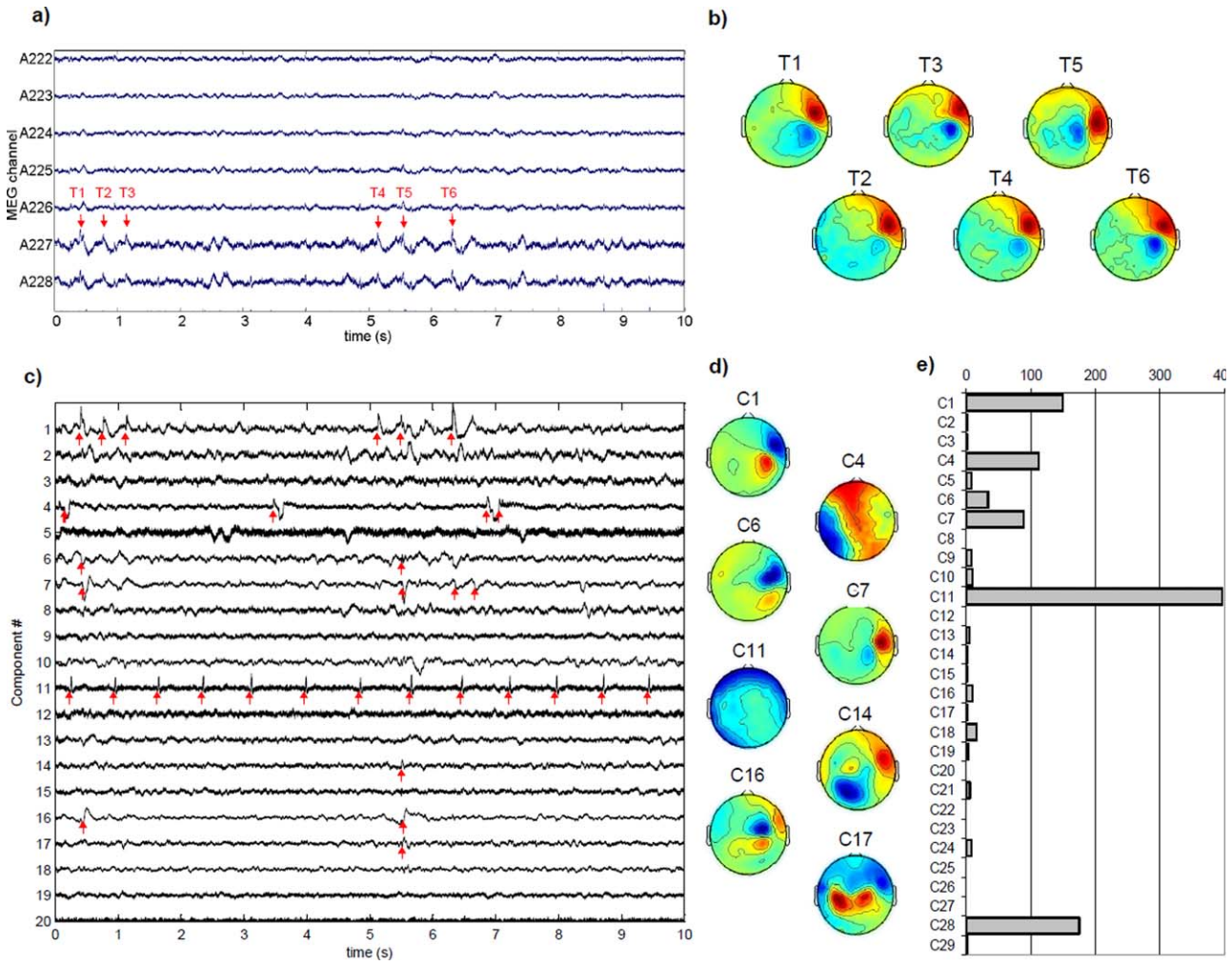

Figure 1.

(**a**) Example of seven channels of original MEG data with visible spikes (patient 1, only 10 s are shown). (**b**) Topographies at selected time stamps (T1–6) (**c**) ICA time courses on the same section (only first 20 components are shown). Spike detections are marked with red arrows. Clear interictal spikes can be seen on components 1, 6, 7, and 16. Component 11 corresponds to cardiac artifact. (**d**) Corresponding spatial components (only a selection is shown). Components 1, 6, and 7 have clear dipolar patterns that correspond to one main source. Component 17 is indicative of bilateral brain sources. (**e**) Histogram of spike detections on ICA components. The higher number of spikes corresponds to the cardiac artifact (component 11). Components 1, 4, 6, 7, and 28 present a large number of detected spikes compared with the other components. [Color figure can be viewed in the online issue, which is available at wileyonlinelibrary.com.]

of high frequencies, components IC4 and IC11 present a high number of detections, even though these are not epileptic discharges. Components IC1, IC6, and IC7 have both dipolar topographies and a high number of detected spikes. Component IC2 has also a dipolar pattern but no detection, and could correspond to a slow wave part of the spike. It is interesting to note that spike-related components were in the first components of the ICA decomposition (which are ranked by energy). In Table II, the spike rates are given for ICA on MEG, across patients. The number of spikes per ICA component ranged from 10 to 397. The mean rate across patients was 0.60 spikes/s in MEG (range 0.1–1.54).

Supporting Information Figure 1 presents an exemplary graph of co-occurrence across ICA components (Patient 1). This graph shows that components ICA1, ICA6, and ICA7 present significant pairwise co-occurrence. In this example, the directionality test (Supporting Information Fig 1b) shows that there is a consistent delay between ICA1 and ICA6, with ICA1 as leader. In terms of independent events (NIE), both ICA1 and ICA7 have higher NIEs than ICA6 (Supporting Information Fig 1c). This suggests that the

TABLE II. Spike rates (spikes per s) after automatic detection, on selected SEEG channels and ICA components

	Average rate (spikes per s)		No. spikes (min–max)	
	SEEG	MEG	SEEG	MEG
Patient 1	1.29 ± 0.19	0.53 ± 0.17	1,143–5,694	34–397
Patient 2	1.44 ± 0.18	0.20 ± 0.07	854–7,638	17–289
Patient 3	0.94 ± 0.13	1.54 ± 0.16	913–6,183	127–268
Patient 4	0.94 ± 0.15	0.67 ± 0.16	910–7,369	84–372
Patient 5	0.92 ± 0.30	0.69 ± 0.09	685–4,211	10–126
Patient 6	0.69 ± 0.13	0.44 ± 0.07	166–5,467	70–224
Patient 7	0.15 ± 0.06	0.10 ± 0.15	29–794	10–376

It is to be noted that for patients 3 and 5, MEG data consist of a concatenation of 2 s sections based on visual detection of spikes.

two regions underlying ICA1 and ICA7 play a leading role in the network. Component 11, corresponding to the ECG artifact, was kept here in order to show that no significant co-occurrence was found with other components, indicating robustness of our statistical method.

Across subjects, 5 to 13 components were selected, with a high number of spikes and a topography indicative of a brain source (see Methods section). The majority of components had a topography indicating one main source. In one case, one of the topographies showed two symmetric sources, indicating a network of two regions with highly correlated time courses.

Spike Detection on SEEG

Spike detection resulted in a large number of contacts with high number of spikes (ranging approximately from 29 to 7,638). The spike rates are given in Table II for SEEG across patients. The mean rate across patients is 0.91 spikes/s (range 0.16–1.44) in SEEG and 0.60 spikes/s in MEG (range 0.1–1.54). Figure 2 illustrates the results in Patient 1. Some detections correspond to very sharp events (e.g., L1-L2 channel), while other detected events are less spiky (e.g., L11-L12). The larger number of spikes was found in electrodes L, PFG and T (Fig. 2c), the first two electrodes being in or close to the dysplastic lesion targeted by the L electrode (Fig. 2b).

MEG and SEEG Connectivity Graphs

Figure 3 presents graphs obtained on MEG and SEEG for three patients. In MEG, each ICA component is represented by the first peak of the corresponding source localization (see Materials and Methods section). The normalized co-occurrence graphs are presented, with the

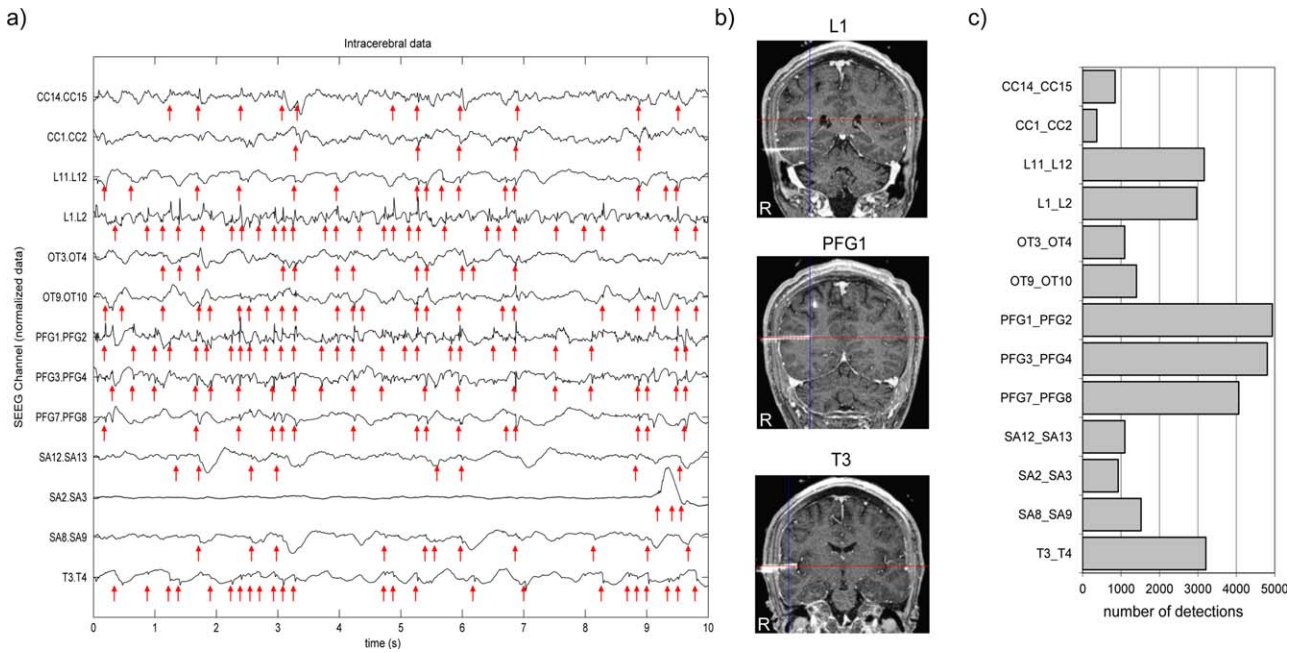

Figure 2.

(**a**) An example of intracerebral EEG (SEEG) data (only 10 s and selected channels are shown), Patient 1. Spike detections are marked with red arrows. One can readily observe that spike density in SEEG is higher than in MEG. (**b**) Registration of CT scan and MRI showing the position of three electrodes out of six. (**c**) Histogram of spike detections. The selected contacts on electrodes PFG, T and L show a higher number of spikes than contacts from other electrodes. [Color figure can be viewed in the online issue, which is available at wileyonlinelibrary.com.]

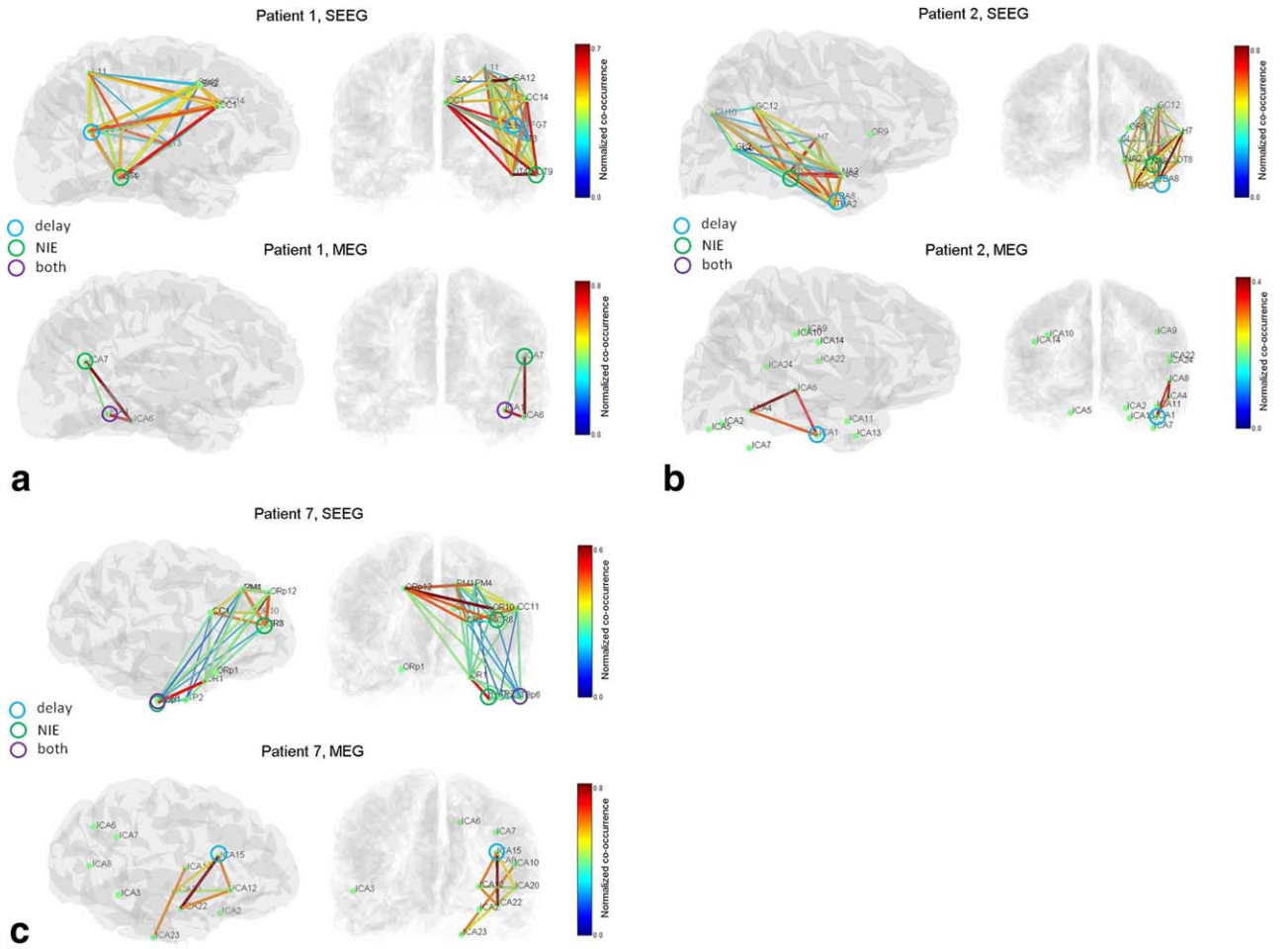

Figure 3.

Interictal co-occurrence networks in SEEG and MEG for three patients. Leading nodes are shown with circles, in the sense of the delay measure, the NIE measure, or both. (**a**) Patient 1. The SEEG graph is more extended than the MEG graph, but share common regions in the parieto-occipital junction and posterior temporal lobe. One leading node is consistent across modalities (temporal posterior region). (**b**) Patient 2. SEEG and MEG network share the posterior temporal regions, and a leader in the lower temporal region with good concordance in the location. (**c**) Patient 7. The general structure of the SEEG network is seen in MEG (basal temporal–frontal network). Only one SEEG leader is identified in MEG. [Color figure can be viewed in the online issue, which is available at wileyonlinelibrary.com.]

leaders as defined by delays or NIE (number of independent events) shown by circles. Results for all patients are summarized in Table III.

Figure 3a illustrates the results of Patient 1. The MEG graph (lower row) involves the right posterior basal temporal region and the right temporo-parieto-occipital junction. The significant delay between ICA1 and ICA6 (Supporting Information Fig. 1b) suggests a short-distance propagation anteriorly in the basal temporal region. The NIE measure (Supporting Information Fig. 1c) indicates that the posterior basal temporal region (ICA1) plays a leading role. The SEEG graph (upper row) also displays these regions, with additional regions in right parietal, right central and right posterior frontal areas. The right posterior temporal region and right temporo-parieto-occipital junction are indicated as leaders on SEEG, suggesting that MEG has detected only one leading region out of two. It is to be noted that the right temporo-parieto-occipital junction was also shown as leader on the MEG NIE graph (Supporting Information Fig. 1c), but was not kept due to our criteria for pruning several links directed towards a common node (see Methods section).

Figure 3b presents the graphs for Patient 2. In MEG, the graph involves the right temporal basal, and right middle lateral temporal regions. The leader as defined by delays is the right temporal basal region (ICA1), suggesting a propagation from anterior to posterior. The SEEG graph shows again a more extended graph, involving also a large

TABLE III. List of network nodes in MEG and SEEG

	Network regions		MEG vs. SEEG		SEEG vs. MEG		Seizure onset	Seizure Propagation	Surgery
	MEG	SEEG	regions	leader	regions	leader	SEEG	SEEG	
1	R post temp (ICA1,6)[a,b]	R post temp (OT4,9)[b]	1	1	1	1		OT lat	
	R parieto-occ -temp junc. (ICA7)	R parieto-occ-temp junc. (PFG7)[a]	1		1	0	PFG med + mid, L med		R post perisylvian
		R sup parietal (L11)			0		L lat		
		R premotor (SA 2,8,12)			0			SA middle	
		R ant cingulate (CC1)			0				
		R temp sup (T lat)			0			T lateral	
2	R temp basal ant (ICA1)[a]	R temp basal ant (TBA2,8)[a]	1	1	1	1	TBA med		Right anterior temp
	R temp post (ICA4)	R temp post (OT 1)[b]	1		1	0	OT med		
		R temp ant med (NA2)			0		NA med		
		R temp post lat (OT 8)			0			OT lat	
	R middle lat temp (ICA8)	R middle lat temp	1		1			H7	
		R occ -temp junction (GL)			0		GL mid		
		R occ-pariet junc. (CU10/GC12)			0			CU lat GC med (R post cing)	
3	L prefrontal (ICA1,2)[a]	L prefrontal (CR5)	1	0	1		CR mid		L prefront
	L central (ICA10)	L central (SC1/7)[a,b]	1		1	0		SC med,lat	
	L medial pariet-occ (ICA8)		NS						
		L premotor (PM5)			0			L premot PM med, lat	
		L insula (H7)			0				
4	R med parieto-occ junc. (ICA4)[a]	R med parieto-occ junction (L5)[a]	1	1	1	1	L medial/middle		R sup calcarine fiss.
		R pariet lateral (PA11)[b]			0	0			
		L pariet medial (PA'1)			0			PA' med	
	L occ-pariet (ICA9)	L occ-pariet (L'5)	1		1			L'5	
	L temp sup (ICA16)		NS						
	L med temp-pariet-occ junction (ICA3)	L med parieto-occ junction (PA')	1		1			PA' med	
		R premotor (SA3)			0				
5		R occ (CU4)			0		CU middle		
	R temp-occ junction (ICA12)[a]	R temp-occ junction (Li8)	1	0	1			LI ext	
	R temp-pariet-occ junc. (ICA13)[a]	R temp-pariet-occ junction (L7)[a]	1	1	1	1	L middle		R Lateral occ-temp
	L temp-occ[b]		NS						
	R middle temp (ICA14)	R middle temp (TO11,C10)	1		1		TO lateral		
	R parieto-occ (ICA18)	R parieto-occ (GC9)	1		1			GC ext	

TABLE III. (Continued)

	Network regions		MEG vs. SEEG		SEEG vs. MEG		Seizure onset	Seizure Propagation	Surgery
	MEG	SEEG	regions	leader	regions	leader	SEEG	SEEG	
	R sup pariet (ICA9)		NS						
	R premotor (ICA24)		NS						
								C medial (hipp. tail) B med (hipp. head), B lat TB med (temporo basal)	
6	L cent (ICA2)	L cent (R6)[a]	1		1	0	R		
	L premotor (ICA20)	L premotor (PM4, M10)[b]	1		1	0	M,G		premotor-prefront
	R cent (ICA13,5)		NS						
		L Thalamus (DM1)			0				
		L operc front (OP2)			0				
		L pariet sup (P10)			0				
7	R basal temp (ICA23)	R basal temp (TBpost1,6) [a,b]	1		1	0		TBpost med	
	R ant temp (ICA 22)	R ant temp (TP2)	1		1		TP2,3	TP med	R ant temp
	R orbito-front (ICA12)	R orbito-front (OR1)	1		1		OR 1,2		R basal frontal
	R prefrontal (ICA15)[a]	R prefront (CR8, CC11,PM1,4, OR10)[b] L prefrontal (ORp12)	1	1	1	1	PM1,2	CR med	R prefront

The concordance of regions between MEG versus SEEG or SEEG versus MEG is listed (1 indicates that a region is one modality is detected in the other).
Temp, temporal; occ, occipital; pariet, parietal; sup, superior; ant, anterior; post, posterior; for SEEG: med: medial (contacts 1–4); mid: middle (contacts 5–8); lat: lateral (contacts 8–12).
[a]The node was defined as leader by the delay criterion.
[b]The node was defined as leader by the NIE criterion.

territory in the right temporo-occipito-parietal region. Both right temporal posterior and right temporal basal regions are defined as leaders, the first region being very consistent spatially between MEG and SEEG.

Figure 3c shows the results of Patient 7. In MEG, the right basal temporal, right anterior temporal and right prefrontal regions are involved. The prefrontal region was seen as leading by the delay criterion. In SEEG, the same regions are detected, with a more widespread involvement of the prefrontal region, including the contralateral homotopic region. The right basal temporal region is defined as leader, contrary to MEG. Still, the location of ICA23 node in MEG (basal temporal) is very consistent with location of leading SEEG contacts.

Table III summarizes the results for all patients. A total of 20 regions (nodes of the graphs) were detected in MEG, whereas 38 regions were detected in SEEG. Six regions in MEG could not be confronted to SEEG as they were not sampled by SEEG electrodes. Regions detected in MEG were confirmed by SEEG (when there was an electrode in the region) in 20 cases out of 20 (100%), and the number of MEG leaders confirmed by SEEG (when regions were sampled) was five of seven (71%). Conversely, regions seen in SEEG were detected in MEG in 20 cases out of 38 (53%); for the leaders, this was the case for 5 out of 12 (42%). The MEG leaders according to the delay criterion were confirmed as SEEG delay leaders in three cases out of seven (43%); for the NIE leaders, this was the case for one case out of two (50%). Only two MEG regions out of eight (25%) were qualified as leader according to both criteria.

It is to be noted that there is a large variability in the intervals between MEG and SEEG exams. This can influence the level of match between MEG and SEEG, as the epileptic networks are expected to vary with time and brain state. The two patients with a high match between SEEG and MEG (patients 5 and 7) correspond to short intervals but the number of patients is too small to make conclusions.

Reproducibility of ICA-Based Networks

In order to assess the reproducibility of the ICA decomposition and of the corresponding networks, we performed the analysis on four runs for patients 1 and 2 (Supporting Information Fig. 2). Components were grouped across runs by visual analysis. We obtained good reproducibility of the networks in three runs out of four for patient 1 (run 1, 3, and 6; in run 2, similar components are found but with different directionality) and for two runs out of four for patient 2 (run 3 and 4).

Confrontation With Ictal Patterns and Surgery

For each patient, we obtained information on the localization of the seizure onset zone (SOZ) and regions of seizure propagation from the SEEG clinical reports. We compared the network regions detected in MEG and SEEG with this clinical information (see Table III). The SOZ was detected by our method as an MEG node (whether leader or not) in 12 cases out of 16 (71%); the detected nodes were labeled as leaders only in 5 cases out of 12 (42%) (involving the delay criterion in five cases, and the NIE in one case) . For SEEG, the SOZ was detected as a network node in interictal activity (whether leader or not) in 16 cases out of 16 (100%) of cases, the MEG nodes were labeled as leaders in 8 cases out of 16 (50%). Propagation areas as defined on SEEG ictal discharges were detected on interictal discharges by our method on MEG in 10 cases out of 20 (50%), and on SEEG in 16 cases out of 20 (80%). We present in Supporting Information Figure 3 measures of epileptogenicity index for patients 1, 2, and 7, which permit to assess the network of structures involved at the onset of seizures [Bartolomei et al., 2008].

We also compared the network regions detected in MEG and SEEG with the volume resected during surgery (Table III, last column). For all patients, all the regions where the operation took place were detected as part of the interictal networks, both in MEG and SEEG. These regions were identified as leader in five cases out of nine (56%) in MEG and six cases out of nine (67%) in SEEG. The resected areas for patients 1, 2, and 7 are shown in Supporting Information Figure 3.

We listed in Table I the ILA classification of postoperative outcome for each patient [Wieser et al., 2001]. All patients experienced improvement (OC ranging above or equal to 4), but none was seizure free. In four patients ranging OC3, four out of five, some regions were labeled as epileptogenic zones on SEEG, but were not operated on (patients 1, 2, 5, 6). Within these regions, three regions out of seven (43%) were detected by MEG. In patient 5, classified OC4, the MEG interictal networks was particularly large (seven regions, three defined as leaders). In the patient classified as OC 2 (patient 4), the EZ region defined on SEEG was operated on, and was detected by MEG as a leader.

DISCUSSION

Intracranial recordings, which still remain the method of reference for presurgical evaluation, show that interictal discharges often involve sets of regions with complex spatio-temporal dynamics [Badier and Chauvel, 1995]. In the present study, we introduced a method for characterizing noninvasively interictal networks from MEG recordings. Our strategy was based on processing continuous data, with a multivariate exploratory method (independent component analysis followed by a semiautomatic detection), which needs minimal interaction with the user, contrary to visual marking and classification of events. Moreover, visual marking of events could miss subtle activity arising from a small area of cortex or from deep

regions, which may be captured with multivariate analysis on large datasets [Kobayashi et al., 2001]. A key novel aspect of our procedure was to investigate relationships between components, based on a co-occurrence measure [Bourien et al., 2004].

Connectivity by Co-occurrence on ICA Components

Surface recordings consist of a summation of signals originating from different regions, each with their own temporal dynamics. Independent component analysis has been introduced in the field of EEG processing, first for removing artifacts [Jung et al., 2000], and shortly afterwards for separating cerebral waves evoked during cognitive paradigms [Jung et al., 2001]. This method was also applied successfully for characterizing different processes involved in epileptic discharges, both in EEG and MEG [Kobayashi et al., 1999; Ossadtchi et al., 2004].

We performed semiautomatic spike detection on the SEEG and ICA traces. We observed overall high spiking rates: apart from the two patients with visual triggering, the average interval between spikes ranged between 1.5 and 10 s. Two factors can be involved. Firstly, the ICA decomposition may improve detection of events. Secondly, the detection procedure is based on filtering followed by thresholding, which can be sensitive to artifacts, resulting in false detections [Bénar et al., 2010]. Automatic detection of epileptiform discharges in electrophysiology [Gotman and Gloor, 1976; Wilson and Emerson, 2002] is a difficult task, because of the variability of patterns encountered across and within patients. Therefore, the effect of detection algorithm on connectivity results should be assessed more thoroughly. We expect that statistics of significance of co-occurrence are robust to moderate level of false positives, which requires further investigation.

Another key part of our approach is to use co-occurrence of detected spikes across components in order to define connectivity. This approach was originally proposed on intracerebral EEG where interictal spikes can be observed either independently in different regions or in a co-occurring manner [Bourien et al., 2005]. This co-occurrence can be used as an indicator that the regions are involved in a network activity. It is interesting to note that such approaches have been also used for measuring synchrony in unit activity across neurons [Bourien et al., 2007; Grammont and Riehle, 2003]. In SEEG recordings in epilepsy, complex configurations of patterns can often be observed, involving very different sets of regions, or spreading from one region to a large set of regions [Badier and Chauvel, 1995].

We investigated the reproducibility of the networks found by ICA and co-occurrence. We found that there was a high level of concordance across ICA topographies across runs, but with some variability on the extracted networks. This suggests that, for better robustness, ICA should be run on higher amounts of data. This could be done either by recordings longer runs, by concatenating runs of data before running ICA or by performing clustering on ICA decompositions across runs [Spadone et al., 2012].

Interictal Discharges Involve Large-Scale Networks

We have found on both MEG and SEEG that interictal discharges can involve remote regions that are acting in synchrony, which constitute a widespread irritative zone. In all patients, at least one region could be identified as leading according to our criteria. The fact we observed in some cases several such leaders suggests that temporospatial distribution can be more complex than the traditional view of a "focus" followed by propagation. The concept of a simple propagation can in fact be questioned too: it is likely that, in order to produce a paroxysmal discharge, the remote region needs to be hyperexcitable.

Such large-scale networks have been already observed in ictal discharges, which may involve from the onset complex interactions between several brain structures [Bancaud and Talairach, 1965; Bartolomei et al., 2001; Kramer et al., 2008]. Our observation of widespread interictal networks is consistent with functional MRI studies showing recruitment of several brain areas [Gotman, 2008]. Functional MRI has full volumic measurements at a high spatial resolution. Still, electrophysiology remains unsurpassed in terms of richness of temporal information (time resolution and spectral content), which in turn places it in a privileged position for defining interactions between nodes of the epileptic network. Several studies have reported in electrophysiology involvement of distinct brain areas in interictal discharges [Bettus et al., 2008; Lin et al., 2009; Merlet and Gotman, 1999; Merlet et al., 1996; Ossadtchi et al., 2005; Tanaka et al., 2010; Wilke et al., 2011]. We present here a novel method for extracting such networks non-invasively, acting in an exploratory manner with minimal user intervention, based on a criterion of co-occurrence. We also performed a systematic comparison with intracerebral EEG, as discussed in the next section.

Confrontation of MEG Results to Intracerebral EEG

Intracerebral recordings typically display much more complex spatio-temporal patterns than surface recordings. Non invasive measurements are less sensitive, as they require activity from a large surface of cortex, with high level of spatio-temporal summation [Cosandier-Rimélé et al., 2008; Tao et al., 2005]. Therefore, a key question is to what extent activity measured directly within the brain can be recorded from non-invasive measurements, and whether such recovered activity is clinically relevant.

We have shown that our approach can detect in all cases a significant proportion of activity visible on SEEG, with a

majority (71%) of MEG leaders identified by SEEG. Of particular interest in the context of presurgical evaluation, we did not obtain "false detections." Indeed, all networks nodes detected by MEG were confirmed by SEEG. This is in line with previous localization reports on EEG, MEG and fMRI, where detected regions have a good concordance with intracerebral findings at the sub-lobar level (i.e., of the order of a few centimeters) [Bénar et al., 2006; Gavaret et al., 2004a; Lantz et al., 2001; Merlet and Gotman, 2001].

Still, it is important to note that a significant proportion of network nodes as identified by SEEG were not detected with MEG, some of which identified as leaders by SEEG. Several factors can lead to a mismatch between activities recorded in separate MEG and SEEG sessions, thus limiting the comparability of the corresponding networks. One factor could be the fact that longer sections of SEEG were analyzed, which can influence the number of regions that are given the chance to give rise to a discharge. A second factor is the delay between MEG and SEEG exams, which can be long in some patients. Indeed, the extent and number of epileptic discharges is expected to vary across time at a large scale (days, months, or years), but also within a day as a function of brain state (arousal, sleep, stress etc...) [Malow et al., 1998; Sammaritano et al., 1991]. The extent can potentially vary also as a function of level of medication (but see [Gotman and Koffler, 1989]). In our study, we selected SEEG recordings performed during daytime, in order to limit potential effects arising from sleep.

Another putatively very important factor is the fact that SEEG has a higher sensitivity than MEG, being direct measures within brain structures. Therefore, one needs to keep in mind that some regions can be missed by non-invasive measurements, and as a consequence avoid over-interpreting the significance of leading regions identified on MEG. Lack of sensitivity was already reported in EEG for mesial temporal sources [Gavaret et al., 2004a; Merlet and Gotman, 1999], frontal sources [Gavaret et al., 2006], or in cases with complex interictal organization [Lantz et al., 2003]. We show here in the context of networks that this can also be the case in MEG for extratemporal regions. Less work has been done on the reliability of measures of direction. It is possible that our results could be improved by using measures of directionality based on non-linear correlation or Granger causality on detected spikes [Franaszczuk et al., 1994].

It is likely that the combination of non-invasive tools (simultaneous EEG-fMRI, simultaneous EEG-MEG) will improve sensitivity for definition of active regions [Daunizeau et al., 2007]. Processing of very large datasets (several runs at once) with less dimensionality reduction, all of which is rendered more and more feasible with increasing computer technology, may also improve results.

Confrontation of MEG with SEEG was based on a visual assessment of anatomical regions, which is subjective. However, automatic labeling could be also problematic because of the sharp boundaries between regions that it imposes. Indeed, if a SEEG node and a MEG node are very close in three-dimensional space but within two regions labeled differently, one may still want to tag them as concordant. Further work is needed in order to develop methods for matching network nodes across modalities [Takerkart, 2012].

The implantation of intracerebral EEG is based on hypotheses on the sites of generation of discharges. Still, there is an issue of spatial sampling, as the number of electrodes has to be kept low. An interesting venue is the possibility to generate ultra-realistic MEG simulations of epileptic networks, based on the actual brain connectivity and on computational models, which would give an actual gold standard for testing methods [Jirsa et al., 2002].

The Independence Constraint

Measuring connectivity (i.e., a form of dependence) across independent components may seem somehow paradoxical. However, several features may preserve validity of this approach. First, the ICA technique relies on a minimization algorithm, resulting in maximally independent components that may still retain some residual dependence. Second, the form of ICA that we used only considers zero-lag dependency (time samples can be shuffled and lead to the same results). Therefore, the existence of propagation lags across sources lowers dependency. Third, we used as a measure of connectivity co-occurrence of transient events, which is a weak form of dependence. In particular, we expect that there is a significant set of events where one source is active and not the other, again lowering dependency.

Still, dependence across sources (i.e. time-courses in different brain regions) can result in components capturing several active regions: if two sources are highly correlated, they can give rise to a single component [Makeig et al., 2004]. In this case, our approach stays valid: these two regions need to be considered as forming a network on their own. It is also possible that two correlated sources are still captured by two components, but with "spilling" of one source onto the other (i.e., cross-talk). This would be more problematic, as it could lower sensitivity in the measurement of time delays across sources. We expect ICA to be robust to some level of correlation across brain sources, as long as there is variability in the link across sources (for example, occurrences when one source is active and not the other); this needs further investigation. Interestingly, in our real datasets, we have observed that most sources have topographies with one strong dipolar pattern; on the retained components, we found bilateral sources only in one component. This is a strong argument in favor of the fact that ICA is indeed capable of isolating single brain generators in most cases [Delorme et al., 2012]. Besides, when two bilateral sources are identified in one component, this is already informative in itself on the existence of a strongly synchronized subnetwork of interictal activity.

Other possible approaches could have been based solely on source localization, without ICA, for example on discharges marked visually on the traces [de Gooijer-van de Groep et al., in press]. Once regions of interest are defined, the time course of these regions could be reconstructed by source localization [Kirsch et al., 2006], and the measures of connectivity applied on these signals [Astolfi et al., 2005; Dai et al., 2012; David et al., 2002; Gross et al., 2001]. Such source localization approach would not need to assume maximal independence across sources. Still, it is to be noted that they could also be penalized by high level of correlation across sources, resulting in possible cross-talk or in appearance of "ghost sources" [Trujillo-Barreto et al., 2004].

Relationships Between Ictal and Interictal Networks

In both clinical and fundamental neuroscience, an important question is the relationship between interictal and ictal activity, which is a complex issue [Asano et al., 2003; Gavaret et al., 2004b; Gotman, 1991; Hufnagel et al., 2000]. There is now a large set of evidence that localization of generators of interictal activity with non-invasive measurements can bring essential information in pre-surgical evaluation [Brodbeck et al., 2010; Gavaret et al., 2004a, 2006; Gotman and Pittau, 2011]. It has been demonstrated that interictal MEG provided additional localization information to video-EEG monitoring in 40% of patients [Pataraia et al., 2004; Paulini et al., 2007]. In malformations of cortical development, basing surgical strategy on interictal rather ictal electrical events—in addition to the MRI definition of the lesional zone—could turn out to be an easier and more successful way [Chassoux et al., 2000; Palmini et al., 1995].

We compared our results obtained on interictal activity with (i) the seizure onset zone and the propagation areas defined during SEEG presurgical evaluation (ii) the regions removed by surgery. In a large proportion of cases, the SOZ defined on the basis of SEEG was part of the detected regions in MEG. In terms of surgery, in all cases the operated regions were detected as a node of the MEG interictal network. For all patients, MEG networks were larger than the region that was operated on, including regions that were not sampled by SEEG in four patients. As patients were not completely seizure free, it is possible that SEEG has missed important nodes of the epileptic network, which are visible in MEG due to its more widespread coverage. The hypothesis that MEG-derived interictal networks can be used in the planning of SEEG needs to be tested on a larger series of patients, with more diversity in terms of surgery results.

Toward a "Primary Irritative Zone"

We have shown here that MEG measurements permit extracting a significant proportion of the interictal networks identifiable in SEEG, together with their temporal interaction. We have used two criteria for defining leading regions, based either on delays or of number of independent events.

For diagnostic purposes, much attention has been devoted so far to the definition of the epileptogenic zone, which is the zone of primary organization of the ictal discharges [Bancaud and Talairach, 1965; Bartolomei et al., 2008]. However, ictal propagation is typically fast and widespread, and the frontier between initiation and propagation can be difficult to establish. In this context, the extraction of interictal networks opens the way to the concept of a "primary irritative zone" consisting of regions presenting interictal discharges independently of other regions [Badier and Chauvel, 1995]. In contrast, the "secondary irritative zone" can be defined as the regions presenting discharges that occur under the dependence of the discharges in the primary regions. The definition of such regions has the potential to become a useful clinical marker in the delineation of the regions to be resected.

In methodological terms, future steps will involve more automated procedures for extracting the primary irritative zone. These methods could combine high-dimensional ICA, automatic classification of components, source localization with minimal interaction from the user. Such minimal interaction is important in a clinical setting, as visual analysis needs training and time, and is operator-dependent. In terms of network definition, further work is needed in order to verify if one can improve the detection of leader by signal processing methods such as granger causality [Brovelli et al., 2004]. In this context, multivariate methods which aim at removing indirect correlations are of particular interest [Kuś et al., 2004].

ACKNOWLEDGMENTS

The authors thank Fabrice Wendling for his help on automatic spike detection. CGB thanks Boris Burle for useful discussions on the NIE criterion.

REFERENCES

Alarcon G, Guy CN, Binnie CD, Walker SR, Elwes RD, Polkey CE (1994): Intracerebral propagation of interictal activity in partial epilepsy: Implications for source localisation. J Neurol Neurosurg Psychiatry 57:435–449.

Asano E, Muzik O, Shah A, Juhász C, Chugani DC, Sood S, Janisse J, Ergun EL, Ahn-Ewing J, Shen C, Gotman J, Chugani HT (2003): Quantitative interictal subdural EEG analyses in children with neocortical epilepsy. Epilepsia 44:425–434.

Astolfi L, Cincotti F, Mattia D, Babiloni C, Carducci F, Basilisco A, Rossini PM, Salinari S, Ding L, Ni Y, He B, Babiloni F (2005): Assessing cortical functional connectivity by linear inverse estimation and directed transfer function: Simulations and application to real data. Clin Neurophysiol 116:920–932.

Badier JM, Chauvel P (1995): Spatio-temporal characteristics of paroxysmal interictal events in human temporal lobe epilepsy. J Physiol 89:255–264.

Bancaud J, Talairach J (1965): La stéréo-électro-encéphalographie dans l'épilepsie. Paris.

Bartolomei F, Chauvel P, Wendling F (2008): Epileptogenicity of brain structures in human temporal lobe epilepsy: A quantified study from intracerebral EEG. Brain 131:1818–1830.

Bartolomei F, Wendling F, Bellanger JJ, Régis J, Chauvel P (2001): Neural networks involving the medial temporal structures in temporal lobe epilepsy. Clin Neurophysiol 112:1746–1760.

Bell AJ, Sejnowski TJ (1995): An information-maximization approach to blind separation and blind deconvolution. Neural Comput 7:1129–1159.

Bettus G, Wendling F, Guye M, Valton L, Régis J, Chauvel P, Bartolomei F (2008): Enhanced EEG functional connectivity in mesial temporal lobe epilepsy. Epilepsy Res 81:58–68.

Bourien J, Bartolomei F, Bellanger JJ, Gavaret M, Chauvel P, Wendling F (2005): A method to identify reproducible subsets of co-activated structures during interictal spikes. Application to intracerebral EEG in temporal lobe epilepsy. Clin Neurophysiol 116:443–455.

Bourien J, Bellanger JJ, Bartolomei F, Chauvel P, Wendling F (2004): Mining reproducible activation patterns in epileptic intracerebral EEG signals: Application to interictal activity. IEEE Trans Biomed Eng 51:304–315.

Bourien J, Sanchez JC, Bellanger JJ, Wendling F, Principe JC (2007): Detection of synchronized firings in multivariate neural spike trains during motor tasks. Conf Proc IEEE Eng Med Biol Soc 2007:5210–5213.

Brodbeck V, Spinelli L, Lascano AM, Pollo C, Schaller K, Vargas MI, Wissmeyer M, Michel CM, Seeck M (2010): Electrical source imaging for presurgical focus localization in epilepsy patients with normal MRI. Epilepsia 51:583–591.

Brovelli A, Ding M, Ledberg A, Chen Y, Nakamura R, Bressler SL (2004): Beta oscillations in a large-scale sensorimotor cortical network: Directional influences revealed by Granger causality. Proc Natl Acad Sci USA 101:9849–9854.

Bénar C-G, Grova C, Kobayashi E, Bagshaw AP, Aghakhani Y, Dubeau F, Gotman J (2006): EEG-fMRI of epileptic spikes: concordance with EEG source localization and intracranial EEG. Neuroimage 30:1161–1170.

Bénar CG, Chauvière L, Bartolomei F, Wendling F (2010): Pitfalls of high-pass filtering for detecting epileptic oscillations: A technical note on "false" ripples. Clin Neurophysiol 121:301–310.

Chassoux F, Devaux B, Landré E, Turak B, Nataf F, Varlet P, Chodkiewicz JP, Daumas-Duport C (2000): Stereoelectroencephalography in focal cortical dysplasia: a 3D approach to delineating the dysplastic cortex. Brain 123:1733–1751.

Comon P (1994): Independent component analysis. A new concept? Signal Process 36:287–314.

Cosandier-Rimélé D, Merlet I, Badier JM, Chauvel P, Wendling F (2008): The neuronal sources of EEG: modeling of simultaneous scalp and intracerebral recordings in epilepsy. Neuroimage 42:135–146.

Dai Y, Zhang W, Dickens DL, He B (2012): Source connectivity analysis from MEG and its application to epilepsy source localization. Brain Topogr 25:157–166.

Daunizeau J, Grova C, Marrelec G, Mattout J, Jbabdi S, Pélégrini-Issac M, Lina JM, Benali H (2007): Symmetrical event-related EEG/fMRI information fusion in a variational Bayesian framework. Neuroimage 36:69–87.

David O, Garnero L, Cosmelli D, Varela FJ (2002): Estimation of neural dynamics from MEG/EEG cortical current density maps: Application to the reconstruction of large-scale cortical synchrony. IEEE Trans Biomed Eng 49:975–987.

de Gooijer-van de Groep KL, Leijten FS, Ferrier CH, Huiskamp GJ: Inverse modeling in magnetic source imaging: Comparison of MUSIC, SAM(g2), and sLORETA to interictal intracranial EEG. Hum Brain Mapp (in press) DOI: 10.1002/hbm.22049.

Delorme A, Makeig S (2004): EEGLAB: An open source toolbox for analysis of single-trial EEG dynamics including independent component analysis. J Neurosc Meth 134:9–21.

Delorme A, Palmer J, Onton J, Oostenveld R, Makeig S (2012): Independent EEG sources are dipolar. PLoS One 7: e30135.

Ebersole JS (1997): Magnetoencephalography/magnetic source imaging in the assessment of patients with epilepsy. Epilepsia 38(Suppl 4):S1–S5.

Fischer MJM, Scheler G, Stefan H (2005): Utilization of magnetoencephalography results to obtain favourable outcomes in epilepsy surgery. Brain 128:153–157.

Franaszczuk PJ, Bergey GK, Kamiński MJ (1994): Analysis of mesial temporal seizure onset and propagation using the directed transfer function method. Electroencephalogr Clin Neurophysiol 91:413–427.

Gavaret M, Badier J-M, Marquis P, McGonigal A, Bartolomei F, Regis J, Chauvel P (2006): Electric source imaging in frontal lobe epilepsy. J Clin Neurophysiol 23:358–370.

Gavaret M, Badier JM, Marquis P, Bartolomei F, Chauvel P (2004a): Electric source imaging in temporal lobe epilepsy. J Clin Neurophysiol 21:267–282.

Gavaret M, McGonigal A, Badier J-M, Chauvel P (2004b): Physiology of frontal lobe seizures: Pre-ictal, ictal and inter-ictal relationships. Supp Clin Neurophysiol 57:400–407.

Gotman J (1991): Relationships between interictal spiking and seizures: Human and experimental evidence. Can J Neurol Sci 18:573–576.

Gotman J (1999): Automatic detection of seizures and spikes. J Clin Neurophysiol 16:130–140.

Gotman J (2008): Epileptic networks studied with EEG-fMRI. Epilepsia 49(Suppl 3):42–51.

Gotman J, Gloor P (1976): Automatic recognition and quantification of interictal epileptic activity in the human scalp EEG. Electroencephalogr Clin Neurophysiol 41:513–529.

Gotman J, Koffler DJ (1989): Interictal spiking increases after seizures but does not after decrease in medication. Electroencephalogr Clin Neurophysiol 72:7–15.

Gotman J, Pittau F (2011): Combining EEG and fMRI in the study of epileptic discharges. Epilepsia 52(Suppl 4):38–42.

Grammont F, Riehle A (2003): Spike synchronization and firing rate in a population of motor cortical neurons in relation to movement direction and reaction time. Biol Cybern 88:360–373.

Gross J, Kujala J, Hamalainen M, Timmermann L, Schnitzler A, Salmelin R (2001): Dynamic imaging of coherent sources: Studying neural interactions in the human brain. Proc Natl Acad Sci USA 98:694–699.

Hufnagel A, Dümpelmann M, Zentner J, SchijnsO, Elger CE (2000): Clinical relevance of quantified intracranial interictal spike activity in presurgical evaluation of epilepsy. Epilepsia 41:467–478.

Jirsa VK, Jantzen KJ, Fuchs A, Kelso JA (2002): Spatiotemporal forward solution of the EEG and MEG using network modeling. IEEE Trans Med Imaging 21:493–504.

Jung TP, Makeig S, Humphries C, Lee TW, McKeown MJ, Iragui V, Sejnowski TJ (2000): Removing electroencephalographic artifacts by blind source separation. Psychophysiology 37: 163–178.

Jung TP, Makeig S, Westerfield M, Townsend J, Courchesne E, Sejnowski TJ (2001): Analysis and visualization of single-trial event-related potentials. Hum Brain Mapp 14:166–185.

Kirsch HE, Robinson SE, Mantle M, Nagarajan S (2006): Automated localization of magnetoencephalographic interictal spikes by adaptive spatial filtering. Clin Neurophysiol 117: 2264–2271.

Knowlton RC, Laxer KD, Aminoff MJ, Roberts TP, Wong ST, Rowley HA (1997): Magnetoencephalography in partial epilepsy: Clinical yield and localization accuracy. Ann Neurol 42: 622–631.

Kobayashi K, James CJ, Nakahori T, Akiyama T, Gotman J (1999): Isolation of epileptiform discharges from unaveraged EEG by independent component analysis. Clin Neurophysiol 110:1755–1763.

Kobayashi K, Merlet I, Gotman J (2001): Separation of spikes from background by independent component analysis with dipole modeling and comparison to intracranial recording. Clin Neurophysiol 112:405–413.

Kramer MA, Kolaczyk ED, Kirsch HE (2008): Emergent network topology at seizure onset in humans. Epilepsy Res 79:173–186.

Kuś R, Kamiński M, Blinowska KJ (2004): Determination of EEG activity propagation: Pair-wise versus multichannel estimate. IEEE Trans Biomed Eng 51:1501–1510.

Lantz G, Grave de Peralta Menendez R, Gonzalez Andino S, Michel CM (2001): Noninvasive localization of electromagnetic epileptic activity. II. Demonstration of sublobar accuracy in patients with simultaneous surface and depth recordings. Brain Topogr 14:139–147.

Lantz G, Spinelli L, Seeck M, de Peralta Menendez RG, Sottas CC, Michel CM (2003): Propagation of interictal epileptiform activity can lead to erroneous source localizations: A 128-channel EEG mapping study. J Clin Neurophysiol 20:311–319.

Lin F-H, Hara K, Solo V, Vangel M, Belliveau JW, Stufflebeam SM, Hämäläinen MS (2009): Dynamic Granger-Geweke causality modeling with application to interictal spike propagation. Hum Brain Mapp 30:1877–1886.

Makeig S, Debener S, Onton J, Delorme A (2004): Mining event-related brain dynamics. Trends Cogn Sci 8:204–210.

Malow BA, Lin X, Kushwaha R, Aldrich MS (1998): Interictal spiking increases with sleep depth in temporal lobe epilepsy. Epilepsia 39:1309–1316.

McGonigal A, Bartolomei F, Régis J, Guye M, Gavaret M, Trébuchon-Da Fonseca A, Dufour H, Figarella-Branger D, Girard N, Péragut JC, Chauvel P (2007): Stereoelectroencephalography in presurgical assessment of MRI-negative epilepsy. Brain 130:3169–3183.

Merlet I, Garcia-Larrea L, Grégoire MC, Lavenne F, Mauguière F (1996): Source propagation of interictal spikes in temporal lobe epilepsy. Correlations between spike dipole modelling and [18F]fluorodeoxyglucose PET data. Brain 119:377–392.

Merlet I, Gotman J (1999): Reliability of dipole models of epileptic spikes. Clin Neurophysiol 110:1013–1028.

Merlet I, Gotman J (2001): Dipole modeling of scalp electroencephalogram epileptic discharges: Correlation with intracerebral fields. Clin Neurophysiol 112:414–430.

Ossadtchi A, Baillet S, Mosher JC, Thyerlei D, Sutherling W, Leahy RM (2004) Automated interictal spike detection and source localization in magnetoencephalography using independent components analysis and spatio-temporal clustering. Clin Neurophysiol 115:508–522.

Ossadtchi A, Mosher JC, Sutherling WW, Greenblatt RE, Leahy RM (2005): Hidden Markov modelling of spike propagation from interictal MEG data. Phys Med Biol 50:3447–3469.

Ossenblok P, de Munck JC, Colon A, Drolsbach W, Boon P (2007): Magnetoencephalography is more successful for screening and localizing frontal lobe epilepsy than electroencephalography. Epilepsia 48:2139–2149.

Page E (1954): Continuous inspection schemes. Biometrika 41:100–115.

Palmini A, Gambardella A, Andermann F, Dubeau F, da Costa JC, Olivier A, Tampieri D, Gloor P, Quesney F, Andermann E (1995): Intrinsic epileptogenicity of human dysplastic cortex as suggested by corticography and surgical results. Ann Neurol 37:476–487.

Pascual-Marqui RD, Michel CM, Lehmann D (1994): Low resolution electromagnetic tomography: A new method for localizing electrical activity in the brain. Int J Psychophysiol 18:49–65.

Pataraia E, Simos PG, Castillo EM, Billingsley RL, Sarkari S, Wheless JW, Maggio V, Maggio W, Baumgartner JE, Swank PR, Breier JI, Papanicolaou AC (2004): Does magnetoencephalography add to scalp video-EEG as a diagnostic tool in epilepsy surgery? Neurology 62:943–948.

Paulini A, Fischer M, Rampp S, Scheler G, Hopfengärtner R, Kaltenhäuser M, Dörfler A, Buchfelder M, Stefan H (2007): Lobar localization information in epilepsy patients: MEG–A useful tool in routine presurgical diagnosis. Epilepsy Res 76: 124–130.

Sammaritano M, Gigli GL, Gotman J (1991): Interictal spiking during wakefulness and sleep and the localization of foci in temporal lobe epilepsy. Neurology 41:290–297.

Schwartz DP, Badier JM, Vignal JP, Toulouse P, Scarabin JM, Chauvel P (2003): Non-supervised spatio-temporal analysis of interictal magnetic spikes: Comparison with intracerebral recordings. Clin Neurophysiol 114:438–449.

Spadone S, de Pasquale F, Mantini D, Della Penna S (2012): A K-means multivariate approach for clustering independent components from magnetoencephalographic data. Neuroimage 62:1912–1923.

Stefan H, Rampp S, Knowlton RC (2011): Magnetoencephalography adds to the surgical evaluation process. Epilepsy Behav 20:172–177.

Takerkart SA, Guillaume T, Bertrand S, Daniele RL (2012): Graph-based inter-subject classification of local fMRI patterns. In: Third International Workshop, MLMI 2012, Held in Conjunction with MICCAI. Nice, France: Springer Berlin Heidelberg. pp 184–192.

Talairach J, Bancaud J (1973): Stereotaxic approach to epilepsy: Methodology of anatomo-functional stereotaxic investigations. Progr Neurol Surg 5:297–354.

Tanaka N, Hämäläinen MS, Ahlfors SP, Liu H, Madsen JR, Bourgeois BF, Lee JW, Dworetzky BA, Belliveau JW, Stufflebeam SM (2010): Propagation of epileptic spikes reconstructed from spatiotemporal magnetoencephalographic and electroencephalographic source analysis. Neuroimage 50:217–222.

Tao JX, Ray A, Hawes-Ebersole S, Ebersole JS (2005) Intracranial EEG substrates of scalp EEG interictal spikes. Epilepsia 46:669–676.

Trujillo-Barreto NJ, Aubert-Vázquez E, Valdés-Sosa PA (2004): Bayesian model averaging in EEG/MEG imaging. Neuroimage 21:1300–1319.

Wieser HG, Blume WT, Fish D, Goldensohn E, Hufnagel A, King D, Sperling MR, Lüders H, Pedley TA; ILAE (2001): ILAE Commission Report. Proposal for a new classification of outcome with respect to epileptic seizures following epilepsy surgery. Epilepsia 42:282–286.

Wilke C, Worrell G, He B (2011): Graph analysis of epileptogenic networks in human partial epilepsy. Epilepsia 52:84–93.

Wilson SB, Emerson R (2002): Spike detection: A review and comparison of algorithms. Clin Neurophysiol 113:1873–1881.